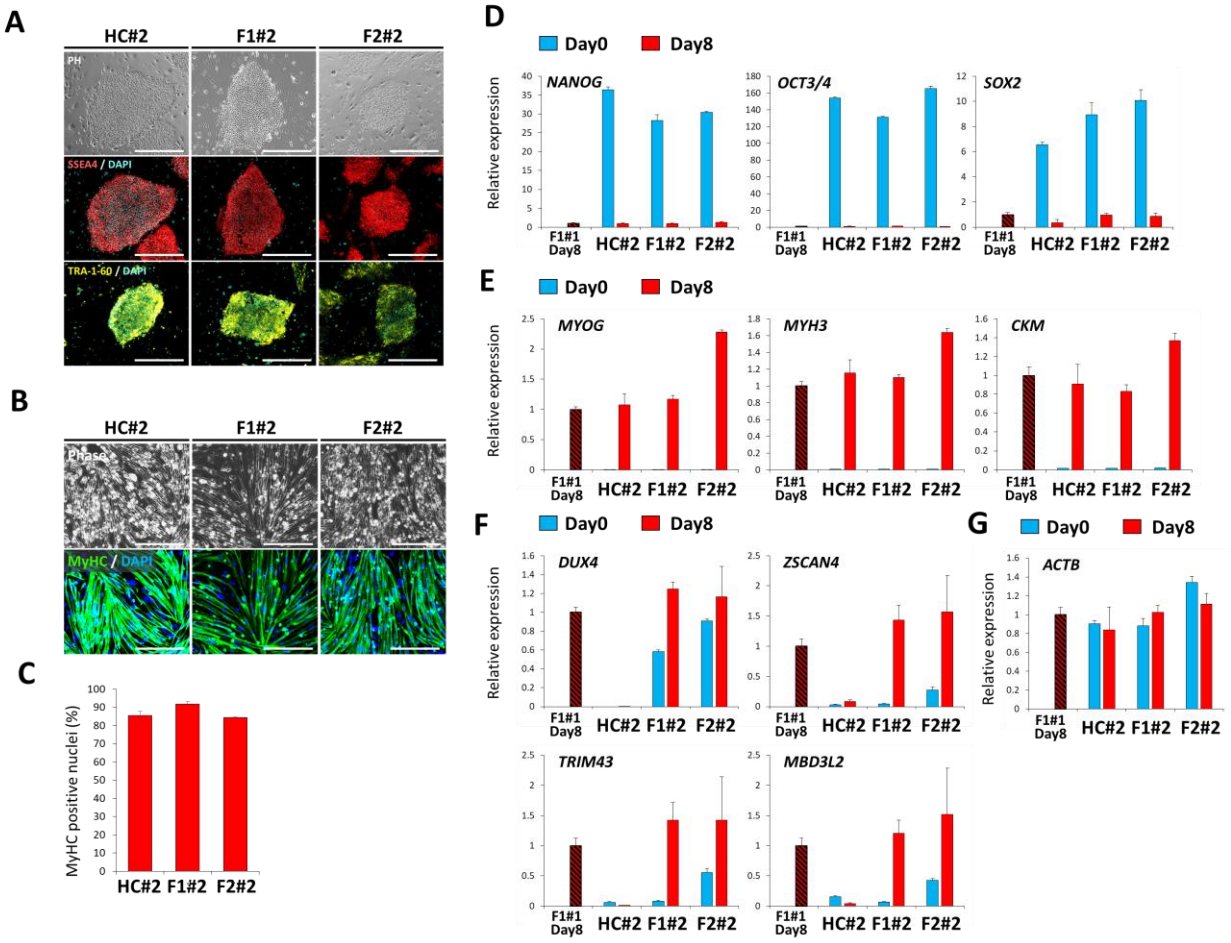

Fig. S1. Additional iPS$^{tet\text{-}MyoD}$ clones were generated from a healthy control, FSHD1 and FSHD2 patients. A. Representative images of immunofluorescence staining of SSEA4 (red) and TRA-1-60 (yellow) in undifferentiated iPSC$^{tet\text{-}MyoD}$ clones. Scale bar: 500 µm. B. Representative images of immunofluorescence staining of myosin heavy chain (MyHC, green) in differentiated myocytes at day 8. Scale bar: 500 µm. C. Differentiation efficiency was quantified by calculating the percentage of MyHC positive nuclei in total nuclei at day 8 (n =4). D-G. RT-qPCR analysis among day0 (undifferentiated) and day8 (differentiated) of each clone (n =3) for D) pluripotency markers, E) myogenic markers, F) DUX4 and its downstream targets and, G) ACTB as a reference gene. Relative expression levels were normalized to RPLP0 as an internal control in each sample and subsequently to F1#1 at day8 (differentiated). Data information: In (D-H), data are represented as mean ± SEM.

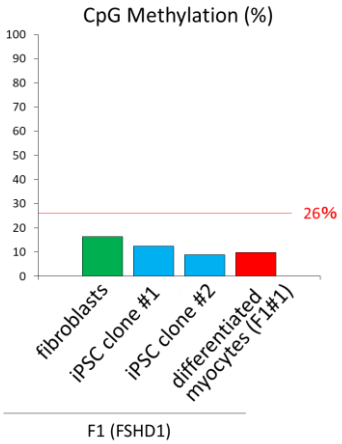

Fig. S2. DNA methylation analysis on D4Z4 region showed stably low states among cell types from the F1 (FSHD1) individual with those levels lower than the previously reported level for non-FSHD allele (26%, refered in (1)). This result implicates that DNA methylation status on D4Z4 region is independent of reprograming process or myogenic differentiation process in FSHD allele.

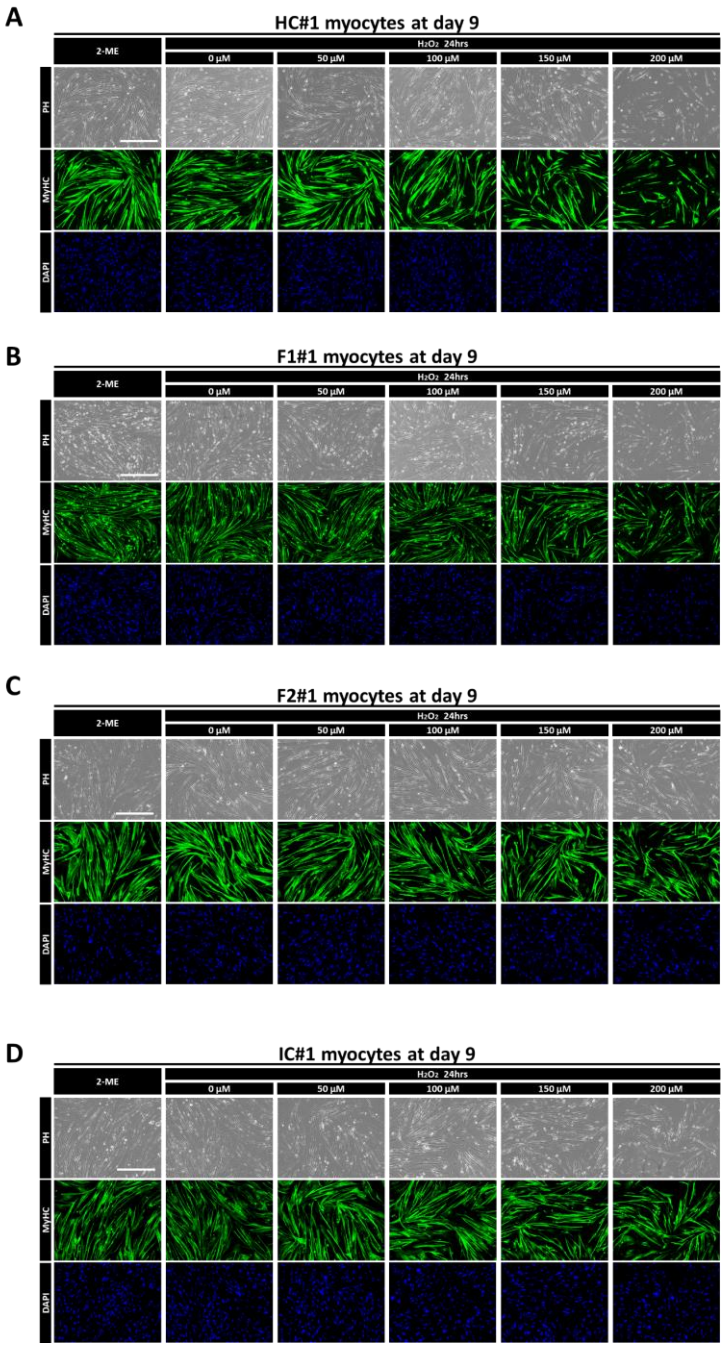

Fig. S3. Representative images of immunofluorescence staining of myosin heavy chain (MyHC, green) in differentiated myocytes of A) HC#1, B) F1#1, C) F2#1, and D) IC#1 incubated with 2-ME or with H_2O_2 at varieties of concentration for 24 hours at day 8. Scale bar: 500 µm. Note that most of the cells show comparable morphology and cell density among the conditions with 0 -100 µM H_2O_2 in each clone.

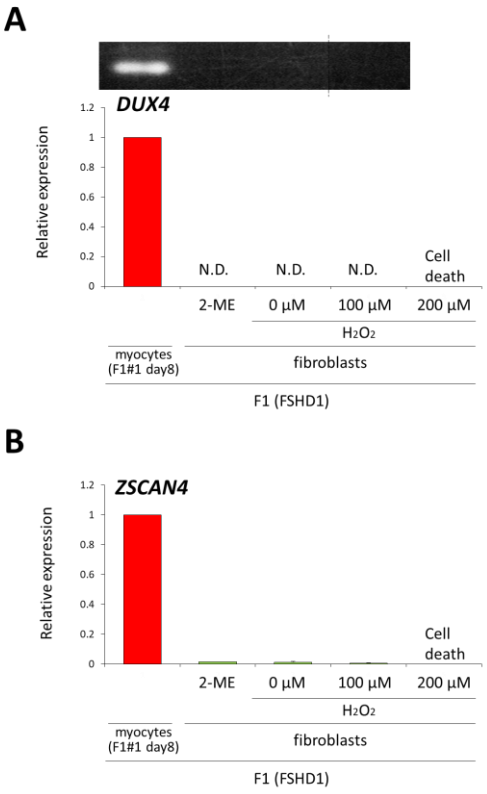

Fig. S4. RT-qPCR analysis showed that FSHD1 (F1) fibroblasts did not express A) DUX4 and B) ZSCAN4 (*n* =3), compared to differentiated myocytes of F1#1. N.D.: not detected. The representative result of electrophoresis of the PCR-products in RT-qPCR analysis for DUX4 is shown above the graph in (A).

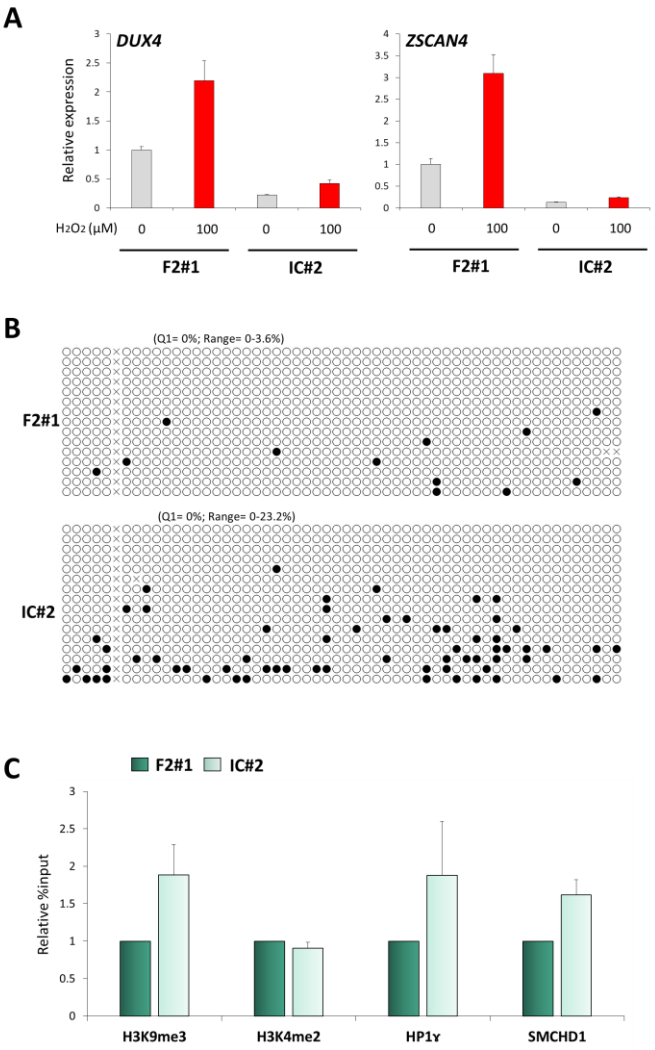

Fig. S5. IC#2 resembled DUX4 increase by oxidative stress and epigenetic features of IC#1, related to Figure 3 and 4. A. RT-qPCR analysis for DUX4 and ZSCAN4 among parental F2#1 myocytes and isogenic control IC#2 myocytes at day 8 in the absence or presence of 100 µM H_2O_2 stimulation for 24 hours (*n* =3). Relative expression levels were normalized to RPLP0 as an internal control in each sample and subsequently to F2#1 without H_2O_2. B. DNA methylation analysis on 4q35. C. ChIP RT-qPCR was performed on 4q35 for H3K9me3, H3K4me2 (as a negative control), HP1ɤ and SMCHD1 (*n* =3). Relative %input was normalized to F2#1. Data information: The data in (A) and (C) are represented as mean ± SEM.

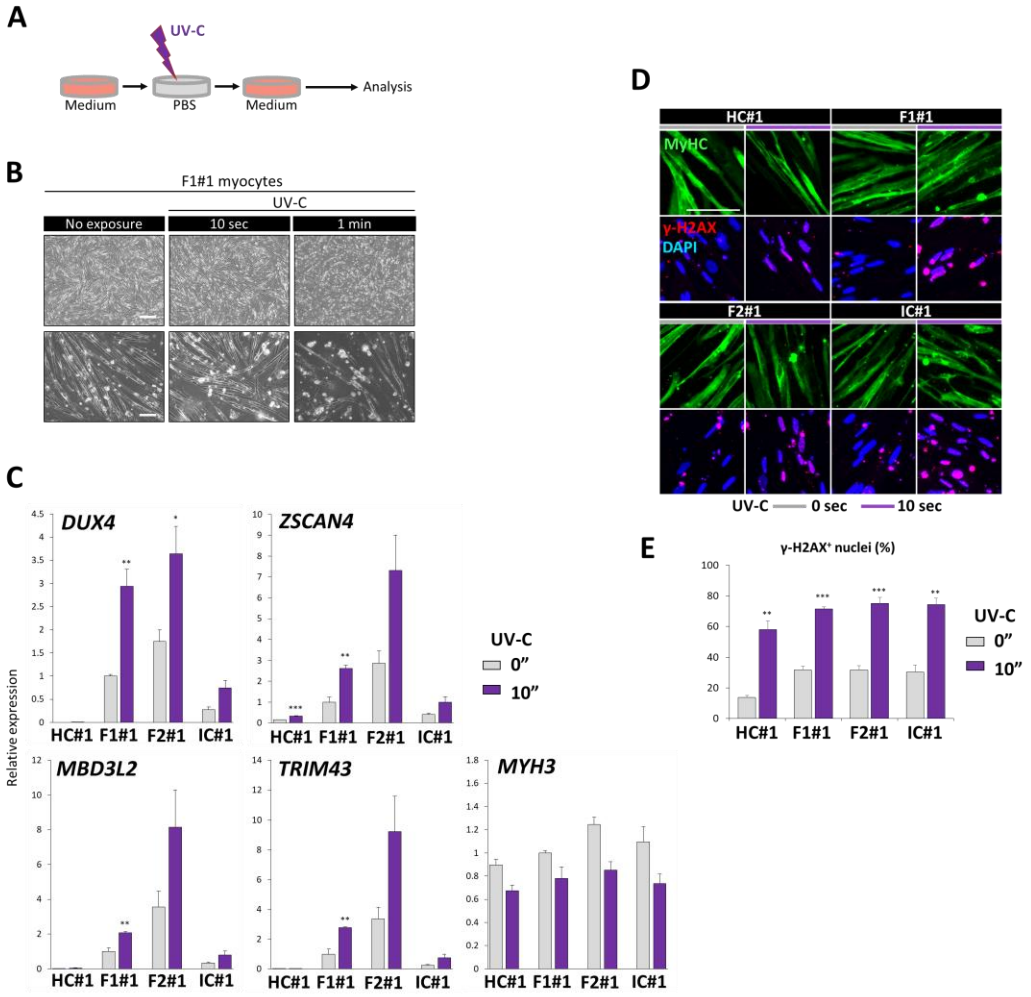

Fig. S6. UV-C exposure increased DUX4 expression. A. Scheme of UV-C exposure. UV-C in the laminar flow cabinet was used. The estimated power is ~1 J/m2・sec. Medium was replaced by PBS at the time of UV-C exposure. Differentiated myocytes, at day 8 after induction, were exposed to UV-C, incubated for 24 or 9 hours, and analyzed. B. Representative phase-contrast images of F1#1 myocytes exposed to UV-C. Exposure to UV-C for 10 seconds, but not one minute allowed most of the cells to be attached on the dish without morphological abnormality 1 day after stimulation. Scale bars: 500 μm for upper panels and 100 μm for lower panels. C. RT-qPCR was performed for DUX4, its downstream targets (ZSCAN4, TRIM43, and MBD3L2), and MYH3 in HC#1, F1#1, F2#1, and IC#1 myocytes exposed to UV-C and incubated for 24 hours (*n* =3 for each condition). Relative expression levels were normalized to RPLP0 as an internal control in each sample and subsequently to F1#1 without UV-C exposure. D. Representative images of immunofluorescence staining of MyHC (green) and ɤ-H2AX (red) of HC#1, F1#1, F2#1, and IC#1 myocytes at day 8 exposed to UV-C. Cells were fixed 9 hours after UV-C exposure. Scale bar: 100 μm. E. The percentages of ɤ-H2AX positive nuclei in total nuclei in (D) (*n* =3). Data information: In (C) and (E), data are represented as mean ± SEM. *P ≤ 0.05, **P ≤ 0.01, ***P ≤ 0.001 (Student's t-test in (C) and (E)).

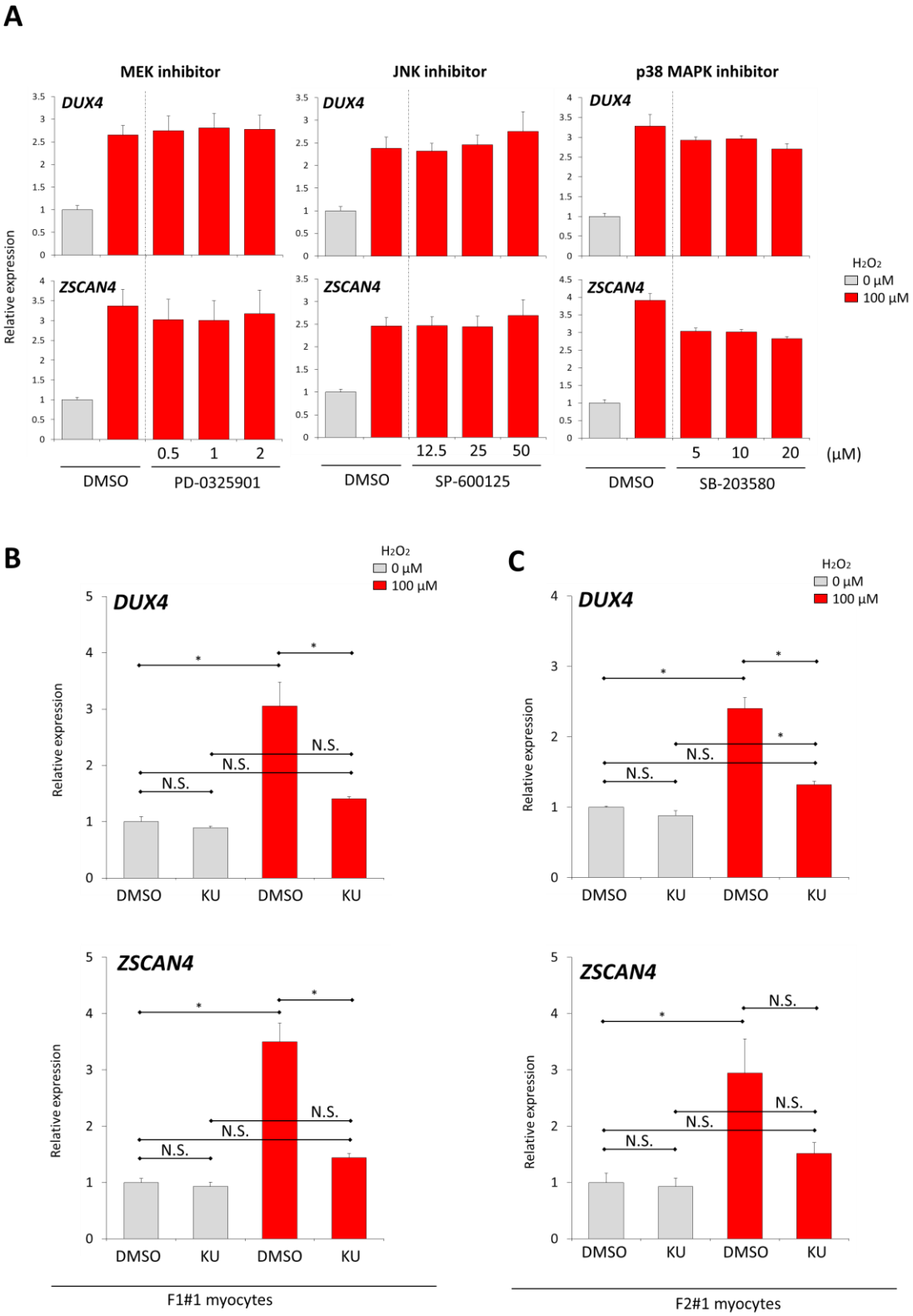
A
MEK inhibitor
JNK inhibitor
p38 MAPK inhibitor
DUX4
ZSCAN4
Relative expression
H2O2
0 μM
100 μM
0.5
1
2
12.5
25
50
5
10
20
(μM)
DMSO
PD-0325901
SP-600125
SB-203580
B
C
KU
N.S.
*
F1#1 myocytes
F2#1 myocytes

Fig. S7. Figure S7. The effect of inhibition of various kinases on DUX4 activity. A) Inhibition of MAPK families did not suppress DUX4 increase by H2O2. RT-qPCR was performed for DUX4 and ZSCAN4 in F1#1 myocytes under H_2O_2 stimulation treated with PD-0325901, SP-600125 or SB-203580 (inhibitors for MEK, JNK, or p38 MAPK, respectively) (n =3 for each condition). Relative expression levels were normalized to RPLP0 as an internal control in each sample and subsequently to the condition with 0 μM H_2O_2. DMSO was added to each sample to keep its final concentration comparable among all the conditions. B-C) Inhibition of ATM did not suppress DUX4 activity in the absence of oxidative stress. RT-qPCR was performed for DUX4 and ZSCAN4 in F1#1 myocytes (B) and F2#1 myocytes (C) in the presence or absence of H_2O_2 stimulation treated with 20 μM KU-55933 (KU) or equal volume of the solvent (DMSO) (n =3 for each condition). Relative expression levels were normalized to RPLP0 as an internal control in each sample and subsequently to the condition with 0 μM H_2O_2 and DMSO. DMSO was added to each sample to keep its final concentration comparable among all the conditions.

Data information: In (A-C) data are represented as mean ± SEM. In (B-C), *P ≤ 0.05, N.S. not significant (One way ANOVA followed by Tukey‘s test)..

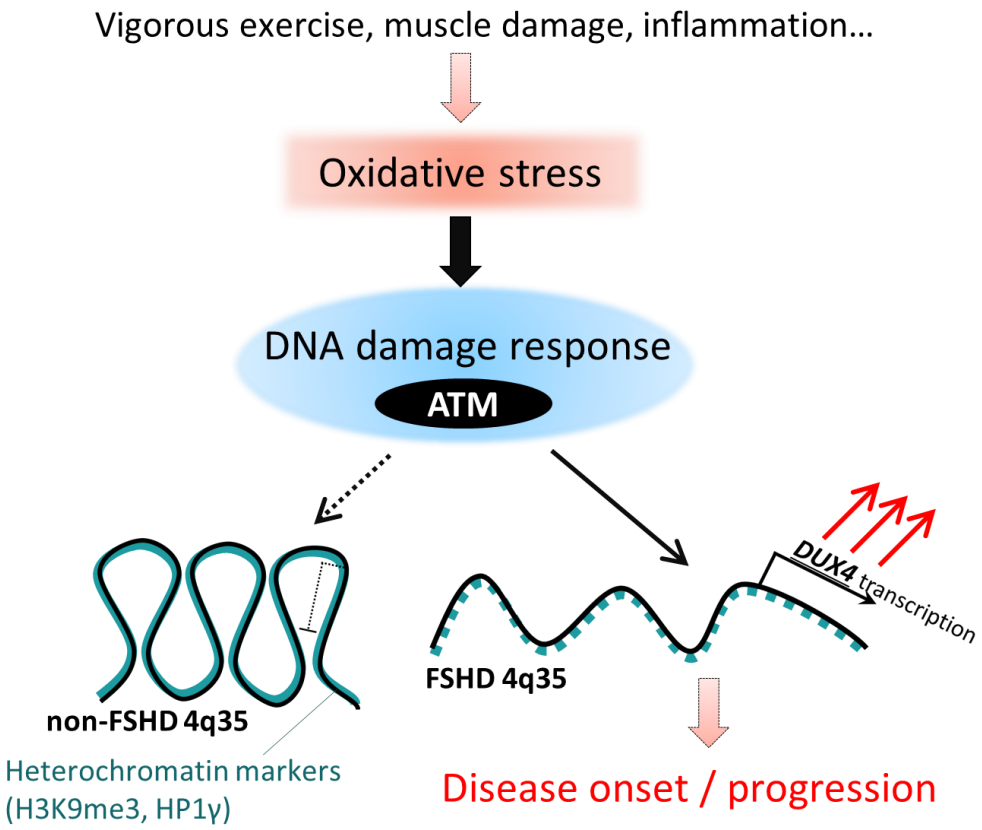

Fig. S8. A model of involvement of oxidative stress in FSHD pathogenesis. Oxidative stress (OS) is a environmental stress which is easy to be triggered by physiological conditions such as extreme exercise, muscle damage or inflammation in skeletal muscle. OS causes transient DNA damage response mediated by ATM signaling, which is kept away from non-FSHD "closed" 4q35 chromatin, but has an aberrant access to FSHD "opened" 4q35 chromatin. This causes up-regulation of DUX4 gene expression and can affect disease onset or progression.

Table S1. Information about the donors for the iPSC establishment.

Donor	Type	Sex	Number of D4Z4 repeats on 4qA allele	SMCHD1 mutation	Age of onset (yrs)	Age of specimen provided (yrs)	origin of cell
F1	FSHD1	Male	3	–	13	26	skin fibroblasts
F2	FSHD2	Female	12	heterozygous g.2750458_2750472del	14	55	blood cells
HC	–	Female	N.D.	–	–	35	skin fibroblasts

Table S2. Primers used for the correction of SMCHD1 mutation in iPSCs

Purpose		
Arm region for HR template	Fw	GAAAGTGAAAGCTTGGTTATCACTG
	Rv	GAAACATCACAATGTAGACTACTC
PCR amplicon for sequencing	Fw	GAGATGGGTTTTAGGATTTGGGAGAA
	Rv	TCCACTCTCTTTCAAGCAGTCTATCA

Table S3. Antibodies used in this study.

1st Antibody	Source	Clonarity	Dilution	Company
Myosin Heavy Chain (MyHC, MF20)	Mouse	Monoclonal	1/800	eBioscience
Stage-Specific Embryonic Antigen-4	Mouse	Monoclonal	1/100	Millipore
TRA-1-60	Mouse	Monoclonal	1/100	Millipore
γ-H2AX (N1-431)	Mouse	Monoclonal	1/800	BD Biosciences
2nd Antibody	Dilution	Company		
Alexa Fluor 488 anti-mouse IgG	1/500	invitrogen		
Alexa Fluor 488 anti-mouse IgG2b	1/500	invitrogen		
Alexa Fluor 568 anti-mouse IgG1	1/500	invitrogen		

Table S4. Primers used in RT-qPCR analysis

	Target		Sequence	PCR condition			Ref
RT-qPCR	ACTB	Fw	CTCTTCCAGCCTTCCTTCC	Denature	95℃	15″	–
		Rv	CACCTTCACCGTTCCAGTTT	Anealing	60℃	60″	
	RPLP0	Fw	AAACGAGTCCTGGCCTTGTCT	Denature	95℃	15″	–
		Rv	GCAGATGGATCAGCCAAGAAG	Anealing	60℃	60″	
	OCT3/4	Fw	GACAGGGGGAGGGGAGGAGCTAGG	Denature	95℃	15″	–
		Rv	CTTCCCTCCAACCAGTTGCCCCAAAC	Anealing	60℃	60″	
	NANOG	Fw	CAGTCTGGACACTGGCTGAA	Denature	95℃	15″	–
		Rv	CTCGCTGATTAGGCTCCAAC	Anealing	60℃	60″	
	SOX2	Fw	GGGAAATGGGAGGGGTGCAAAAGAGG	Denature	95℃	15″	–
		Rv	TTGCGTGAGTGTGGATGGGATTGGTG	Anealing	60℃	60″	
	MYOG	Fw	TGGGCGTGTAAGGTGTGTAA	Denature	95℃	15″	–
		Rv	CGATGTACTGGATGGCACTG	Anealing	60℃	60″	
	MYH3	Fw	GCAGATTGAGCTGGAAAAGG	Denature	95℃	15″	–
		Rv	TCAGCTGCTCGATCTCTTCA	Anealing	60℃	60″	
	CKM	Fw	ACATGGCCAAGGTACTGACC	Denature	95℃	15″	–
		Rv	TGATGGGGTCAAAGAGTTCC	Anealing	60℃	60″	
	DUX4	Fw	CCTGGGATTCCTGCCTTCTA	Denature	95℃	30″	54
		Rv	AGCCAGAATTTCACGGAAGA	Anealing	62℃	45″	
	ZSCAN4	Fw	GTGGCCACTGCAATGACAA	Denature	95℃	15″	54
		Rv	AGCTTCCTGTCCCTGCATGT	Anealing	60℃	60″	
	MBD3L2	Fw	CGTTCACCTCTTTTCCAAGC	Denature	95℃	15″	54
		Rv	AGTCTCATGGGGAGAGCAGA	Anealing	60℃	60″	
	TRIM43	Fw	ACCCATCACTGGACTGGTGT	Denature	95℃	15″	54
		Rv	CACATCCTCAAAGAGCCTGA	Anealing	60℃	60″	